The Electron Localization Function in Excited States: The case of the ultra-fast proton transfer of the salicylidene methylamine.

Boris Maulen[1], Andrea Echeverri[1], Tatiana Gómez[2], Patricio Fuentealba[1,3] and Carlos Cárdenas[1,3]*

1. *Departamento de Física, Facultad de Ciencias, Universidad de Chile, Casilla 653, Santiago, Chile. cardena@uchile.cl*
2. *Instituto de Ciencias Químicas Aplicadas, Theoretical and Computational Chemistry Center, Facultad de Ingeniería, Universidad Autónoma de Chile, Av. El Llano Subercaseaux 2801, San Miguel, Santiago de Chile.*
3. *Centro para el Desarrollo de la Nanociencia y la Nanotecnología (CEDENNA), Avda. Ecuador 3493, Santiago 9170124, Chile.*

Abstract.

The physical characterization of the chemical bond in the ground state has been a central theme to theoretical chemistry. Among many techniques, quantum chemical topology (QCT) has emerged as a robust technique to understand the features of the chemical bond and electron organization within molecules. One consolidate tool within QCT is the topological analysis of the electron localization function (ELF). Most research on ELF and chemical bond has focused either on singlet ground states or the first excited triplet. However, most photochemical reactions and photophysical processes occur in excited states with the same spin-symmetry as the ground state. In this work, we develop a proposal on how to compute the ELF in excited states of any symmetry within linear-response time-dependent density functional theory. Then, we study the evolution of the chemical bonds in the ground and excited state intramolecular proton transfer (ESIPT) of a prototypal Schiff Base (the salicylidene methylamine, Scheme 1). We found that the topological analysis of the ELF along reaction paths explain the presence of a barrier for the proton transfer in the ground state and the absence of it in the excited state. Briefly, in the ground state, the cleavage of the O-H bond results in a structure with high electrostatic potential energy due to an excess of electron lone-pairs (3) in the Oxygen atom, which explains the barrier. In the excited state, the electronic transition promotes an enhancement of the basicity of Nitrogen by allocating three nonbonding electrons in

the basin of its lone-pair. This excess of electrons in the N exerts an electrostatic attraction of the proton, which we suggest as the primary driven-force of the barrierless reaction. Because in excited states the molecule can develop more vibrational kinetic energy than in the ground state, we perfumed an ab initio molecular dynamics of the proton transfer in the excited state and corroborate that our conclusions on the topology of the ELF do not change due to dynamic effects.

1. Introduction

Photochromic materials are one of the essential building blocks for improving optically driven molecular memories, optical recording media, photoswitches, light-modulating and data processing materials.[1-7] The excited-state dynamics of these materials makes them attractive to theory and experiments. Upon excitation, these materials could experience photochemical reactions such as ring closure-ring opening, E-Z isomerization, and excited state intramolecular proton transfer (ESIPT). Of particular interest are, because of their potential applications in optoelectronic devices, organic compounds with an intramolecular hydrogen bond (IMHB) that exhibit an ultrafast ESIPT reaction. The essential features for a molecule undergoing ESIPT are the sub-picosecond timescale of the proton transfer, high fluorescence efficiency, and a significant Stokes shift in the absorption-emission spectra. The large Stokes shift, which is a common feature of systems with significant geometry differences between their ground and emissive excited state, is a crucial parameter to design optical materials because it diminishes the self-absorption and light scattering effects.

The design and study of ESIPT chromophores have heavily focused on hydrogen-bonded Schiff bases. These compounds have a complex dynamics on the electronically excited states that can be tuned by structural modifications.[8-23] Examples of those modifications are chemical changes that increase the aromaticity of the substituents groups and electron-donor and electron-acceptor substitutions at the aromatic rings. Different experimental strategies to spectral-tuning the ESIPT emission length are available, which include the extension of conjugation length and structural modification on the aromatic or heterocyclic rings.[11-12, 24-27] On the theoretical side, Nagaoka et al.[28-32] proposed a nodal-plane model, which emerges as a valuable tool to investigate dynamic processes in low lying excited states. Despite significant research on these subjects, aspects regarding the evolution of electronic structure and chemical bonding during the proton transfer dynamics still require investigation.[33] This work introduces an extension of the electron localization function (ELF)[34] to characterize chemical bonding in excited states[35] with the same spin symmetry as the ground state. Then, the topological analysis of the ELF is used to rationalize the evolution of the chemical bonds along the ESIPT of a prototype Schiff base, the salicylidene methylamine (SMA. Scheme 1). The ELF and its

topology provide a physical explanation of why the proton transfer is unlikely in the ground state, but it goes without a barrier in the excited state.

There is a widely accepted mechanism for the relaxation pathways of photochromic Schiff bases (see Scheme 1).[10, 12, 15, 18, 20, 33, 36-88] . Upon excitation from the ground state (S_0) of the *cis*-enol form of the SMA, the first singlet excited state depopulates through several pathways. *i)* A radiative emission from the locally excited enol form. *ii)* The ESIPT process to produce the fluorescent S_1-*cis*-keto. *iii)* Isomerization of the C-C bond in the S_1-*cis*-keto that results in an internal conversion (IC), via a second conical intersection (CI), to either *trans*- or *cis*-enol photochromic forms in S_0. *iv)* Isomerization of the C=N bond which decays via a second CI to the form S_0-*trans*-keto. Finally, due to the low reverse proton transfer energy barrier in S_0, the *cis*-keto form transfers back the proton to form the enol tautomer again, closing the photochemical cycle allowing a new photoactivation process to start over. This work focuses only on the changes of the bond topology in the ESIPT.

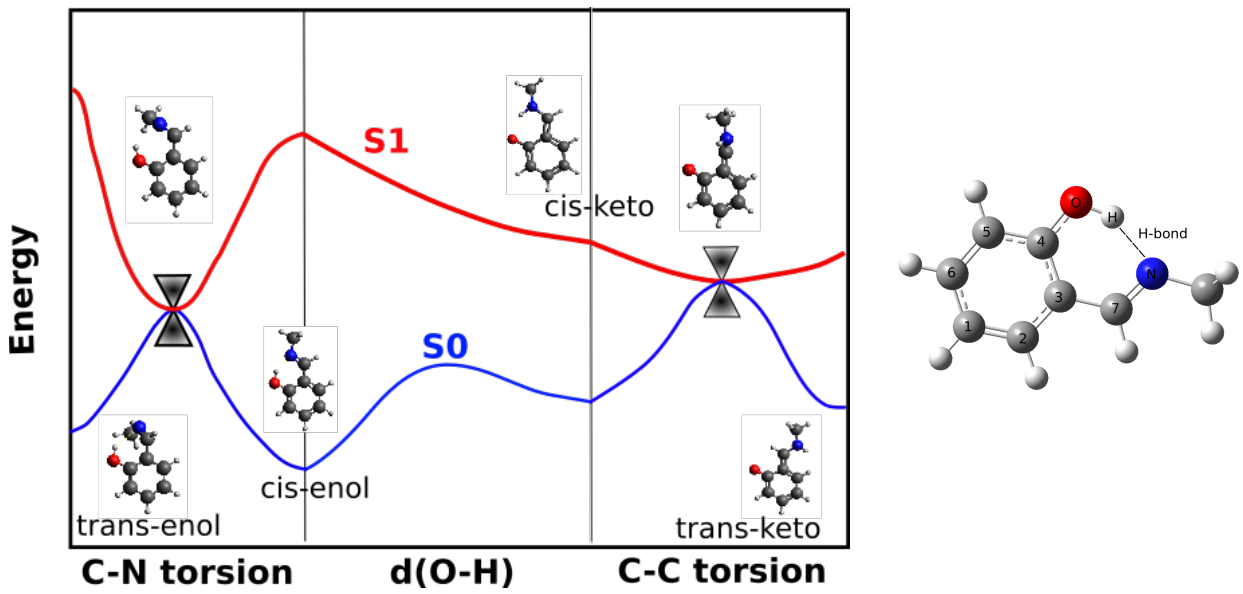

Scheme 1. Diagram of the photo-chemical(-physical) relaxation pathways of the salicylidene methylamine (SMA) and its molecular structure.

2. Theoretical Methods

2.1 ELF in ground states.

Becke and Edgecombe originally defined the ELF for a monodeterminantal Hartree-Fock (HF) wavefunction.[34] Later, Savin showed that its operational definition also holds for ground state density functional theory (DFT).[89] In the ground state, the ELF admits two interpretations: *i*) the ELF is high in those regions where is highly likely to find localized pair of electrons, and *ii)* the ELF is high in those regions where the "excess" of kinetic energy due to the Pauli exclusion principle is small.[89-90] The first interpretation comes from the original definition of ELF,

$$\eta(\mathbf{r}) = \left(1 + \left(\frac{D(\mathbf{r})}{\frac{3}{5}\left(6\pi^2\right)\rho(\mathbf{r})^{5/3}} \right)^2 \right)^{-1} , \qquad (1)$$

where the critical element, $D(\mathbf{r})$, is the curvature of (conditional-) density of probability to find two electrons with the same spin at a (spherical-) averaged distance *s* around a point **r** given that the position of one of them is known with certainty

$$D(\mathbf{r}) = \frac{1}{2}\nabla_s^2 \left(\frac{\pi^{\sigma\sigma}(\mathbf{r},\mathbf{r}+\mathbf{s})}{\rho(\mathbf{r})} \right)_{\mathbf{s}=\mathbf{0}} = \frac{1}{2}\nabla_s^2 P^{\sigma\sigma}(\mathbf{r},\mathbf{r}+\mathbf{s})\Big|_{\mathbf{s}=\mathbf{0}} = \left(\sum_i^{\sigma} \left|\nabla\psi_i(\mathbf{r})\right|^2 - \frac{1}{4}\frac{\left|\nabla\rho^{\sigma}(\mathbf{r})\right|^2}{\rho^{\sigma}(\mathbf{r})} \right) , \qquad (2)$$

where $\pi^{\sigma\sigma}(\mathbf{r},\mathbf{r}+\mathbf{s})$, $\{\psi_i\}$, and $\rho^{\sigma}(\mathbf{r})$ are the same-spin (σσ) two-particle density matrix (2PDM), the occupied molecular orbitals (with spin σ) of a HF wavefunction, and the density of electrons with σ spin. The smallest the probability of finding two electrons with the same spin in a region, the more localized is the reference electron. The second interpretation raises because the first term of $D(\mathbf{r})$ is half the positive-definite kinetic energy density of a system with mean-field-interacting electrons, $\tau(\mathbf{r})$, while the second is half the kinetic energy density of a system of bosons with the same density. Therefore, electrons do not localize where $D(\mathbf{r})$ is large because the Pauli principle imposes them

high kinetic energy. This last interpretation is especially crucial in DFT because it allows the use of Kohn-Sham (KS) orbitals in Eq. (2) even though its original definition holds for an HF wavefunction.

2.2 ELF in excited states.

Excited states could be divided into two kinds, those with the same spin symmetry as the ground state and those with different symmetry. The first is the most relevant to the photochemistry of organic molecules because the absence of strong spin-orbit coupling forbids the transition between states with different spin symmetry. Evaluating the ELF of states of different symmetry, with Eq. (1), is not a problem at all because DFT-KS is enough to compute the properties of the lowest excited state of a given spin multiplicity. Computing the ELF of a molecular system in different spin states is customary.[91] On the contrary, we are not aware of any work that focuses on the ELF of an excited state of the same spin symmetry as the ground state. A plausible explanation for this lack of research, it is that the broadly used working equation for computing the ELF (last term of Equation (2)) holds for monodeterminantal wavefunctions, while accessing to the wavefunction of an excited state usually requires MRSCF methods. Indeed, the ELF is calculable with any method the curvature of the 2PDM is available for.[92-96] However, the evaluation of the curvature of the 2PDM is tedious and computationally expensive, so it can be performed only for small molecules.[97] Still, to explore the bond pattern and its dynamical evolution in medium and sizeable molecular system, one should resort in computationally affordable methods for the excited state. A suitable balance between accuracy and computational cost is time dependent-DFT in the linear regime (LR-TDDFT).[98] However, LR-TDDFT does not provide a 2PDM of the excited state but only the one-particle density matrix (1PDM). Despite the formal definition of the ELF requires the curvature of the 2PDM, in its original work, Becke and Edgecombe[34] reconstructed the 2PDM in terms of the 1PDM (which is essential to the HF approximation). Here we propose such reconstruction for the 2PDM of k-th excited state in terms of the natural orbitals (NO) of a given spin σ, $\left\{\phi_{i,\sigma}\right\}$, and the occupation numbers, $\{n_{i,\sigma}\}$,of the 1PDM of the of k-th excited state:

$$\pi^{\sigma\sigma}_{(k)}(\mathbf{r}_1,\mathbf{r}_2)=\sum_i\sum_j n_{i,\sigma}n_{j,\sigma}\left(\phi^{(k)*}_{i,\sigma}(\mathbf{r}_1)\phi^{(k)}_{j,\sigma}(\mathbf{r}_2)\phi^{(k)*}_{i,\sigma}(\mathbf{r}_1)\phi^{(k)}_{j,\sigma}(\mathbf{r}_2)-\phi^{(k)*}_{i,\sigma}(\mathbf{r}_1)\phi^{(k)}_{j,\sigma}(\mathbf{r}_2)\phi^{(k)*}_{j,\sigma}(\mathbf{r}_1)\phi^{(k)}_{i,\sigma}(\mathbf{r}_2)\right), \quad (3)$$

with which the ELF of the k-th excited state is readily evaluated from Eq. (2),

$$\eta^{(k)}(\mathbf{r})=\left(1+\left(\frac{\sum_i n_{i,\sigma}\left|\nabla\phi^{(k)}_{i,\sigma}(\mathbf{r})\right|^2-\frac{1}{4}\frac{\left|\nabla\rho^{\sigma,(k)}(\mathbf{r})\right|^2}{\rho^{\sigma,(k)}(\mathbf{r})}}{\frac{3}{5}\left(6\pi^2\right)\rho^{\sigma,(k)}(\mathbf{r})^{5/3}}\right)^2\right)^{-1}. \quad (4)$$

Although this expression looks quite similar to the ELF for ground states there are substantial differences: *i)* the density corresponds to the *k-th* excited state, *ii)* the orbitals $\{\phi_i\}$ are those that diagonalize the excited state 1PDM, and *iii)* the sum goes over all NO and not just occupied KS orbitals of the ground state.

The reconstruction of the 2PDM in terms of NO to compute the ELF in the ground state has been attempted before. Remarkably, Matito et al.[99] showed that reconstructions of the 2PDM with NO are exceptionally accurate to include correlation effects in the ELF of medium to highly correlated systems. In their work, they show that an HF-like reconstruction (Eq. (3)) is exceptionally accurate to include correlation effects in the ELF. They also conclude that for the calculation of two-particles topological properties such as the covariance of the population of the basins of the ELF, the accuracy holds only for systems with moderate correlation. It is worth mentioning that the HF-reconstruction is the most straightforward reconstruction of the 2PDM, and that density matrix functional theory provides us with many other reconstructions that aim to include correlation effects.[100] We will focus in the HF-like reconstruction because it is known that all that is need it for the ELF to capture the bonding in molecules is the inclusion of the Pauli principle, which is captured by the kinetic energy density ($\tau(\mathbf{r})=\sum_i n_i\left|\nabla\phi_i(\mathbf{r})\right|^2$). Finally, it was already two decades ago that Andreas Savin suggested that the ELF could be evaluated in terms of NO's.[101] Further exploration on the consequences of the type of reconstruction of the 2PDM in terms of NO is an o going project.

2.3 Computational details.

All structural optimizations in the ground and excited states were done with DFT and TD-DFT methodologies using the long-range corrected hybrid density functional of Head-Gordon et al.[102] ωB97X-D and the split-triple-valence basis set 6-311+G(d,p). The ωB97X-D functional was chosen because it is a hybrid functional with range separation that employs 100% of Hartree-Fock-type exchange (EXX) for the long-range electron-electron interaction. The advantage of this functional is that it recovers the correct long-range *1/r* behaviour of the exchange potential while its computational cost is similar to standard functionals. Having a correct description of the long-range piece of the exchange is essential to describe excitations with charge transfer character. Although The SMA has little charge transfer in the $S_0 \rightarrow S_1$ excitation, more pronounced charge transfer could happen in other sectors of the excited state potential energy surface (PES) visited during the proton transfer.

Possible dynamics effects on the topology of the ELF in the excited state were studied by performing a Born-Oppenheimer ab initio molecular dynamics in the micro-canonical ensemble in S_1. All the trajectories started from the FC structure, and only the velocities were randomly sampled from a Boltzmann distribution of 300 K. The equation of motion were integrated with the Velert-velocity algorithm with a time step of 0.5 fs and 150 fs of total simulation time. The forces on atoms were computed with TD-DFT with the ω-B97XD exchange correlation functional. The KS orbitals were expanded in two types of basis sets: a 6-311++G(d,P) for the atoms of the ring involved in the proton transfer (O,N,H, C3,C4,C7 in Scheme 1), and a 6-31+(d,p) for the rest. All electronic structure calculations were done with Gaussian 09.[103] The ELF and its topology were calculated with TopMod.[104] In the case of the excited state, we tested the results by computing the ELF in our implementation in HORTON and ChemTools.[105]

3. Results and discussion.

We first discuss the evolution of the topology of the ELF along the proton-transfer path in the ground state of the SMA. Then we will do the same for the excited state, and by comparing both cases, we elaborate a physical explanation of why the transfer occurs

without a barrier in the excited state. We also study possible dynamic effects on the topology of the ELF by performing molecular dynamics on the excited state.

3.1 ***Ground state.***

The PES along the IRC of the proton transfer and snapshots of localization domains of ELF=0.8 at the enol, keto, and the transition state (TS) are shown in Figure 1. We call the attention to the domains of the ELF around the hydrogen bond. At the enol and keto, the hydrogen forms a covalent bond with O and N, respectively. Those bonds correspond to disynaptic basins V(O-H) and V(H-N). At the transition state, the H and N belong to the same localization domain, which indicates that the O-H bond has already broken. However, as it will be seen, the N-H bond is not yet formed. Interestingly, before the TS there is a region where the H has an own monosynaptic basin, V(H), and it is neither bonded to the N nor the O. At the distance r_{OH}=*1.2 Å*, the correlation between H and O and between H and N equals, and we call this point an *electronic transition state.* By equal correlation, we mean that the covariance[90, 106] of the population of the basin V(H) with the non-bonding basins of N, V(N), and the one left behind in the O, V(O1), after O-H bond breaking, are the same.

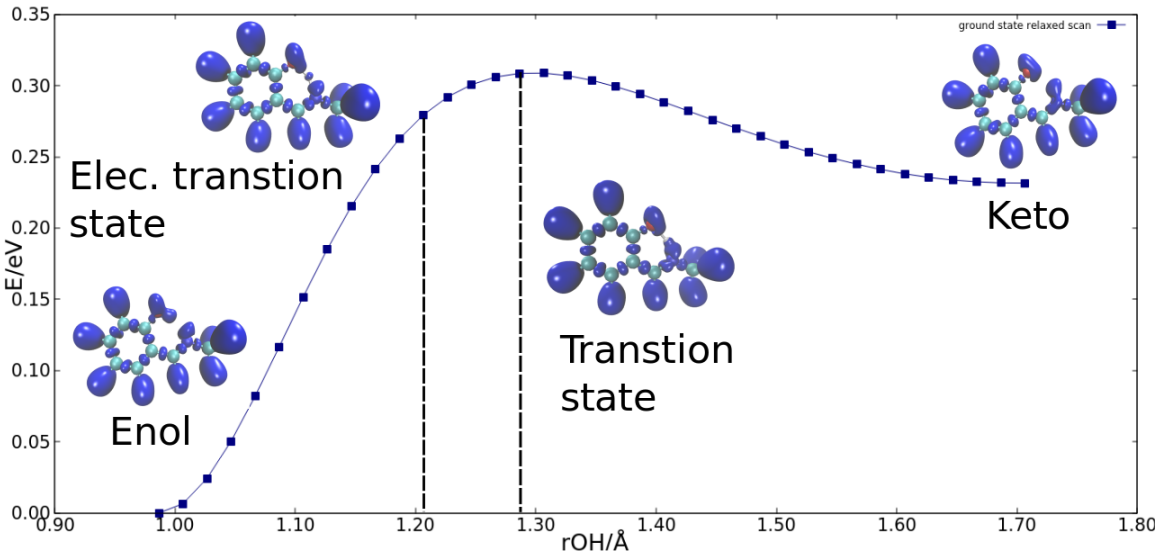

Figure 1. Potential energy surface along the Internal reaction coordinate of the proton transfer in the ground state of the SMA. Insets are isosurfaces of ELF=0.8. Besides the ELF in the enol and keto, the ELF in the transition state and the so-called electronic-transition state are also shown. The energy origin corresponds to the energy of the enol tautomer.

Several catastrophes in the topology of ELF occur as the proton transfers proceeds. These catastrophes are the disappearance and emergence of basins, which indicates, for instance, bond breaking and formation. Two catastrophes arise in the ground state. One happens at r_{OH}=*1.12 Å,* and it represents the breaking of the O-H (see Figure 2). That is, the basin V(O,H) disappears, leaving behind the monosynaptic basins V(O1) and V(H). The V(O1) basin corresponds to an incomplete extra lone-pair in the oxygen (1.4 electrons (*e*)). The V(H) corresponds to a proton dressed with 0.45 *e* that persists between r_{OH}=*1.12 Å* and r_{OH}=*1.40 Å*. Hence, the proton-transfer occurs via a pseudoatomic form of the proton, and the rupture of the O-H bond and the formation of the N-H are not simultaneous. Notice also that the rupture of the O-H bond occurs before the TS (r_{OH}=*1.28 Å*).

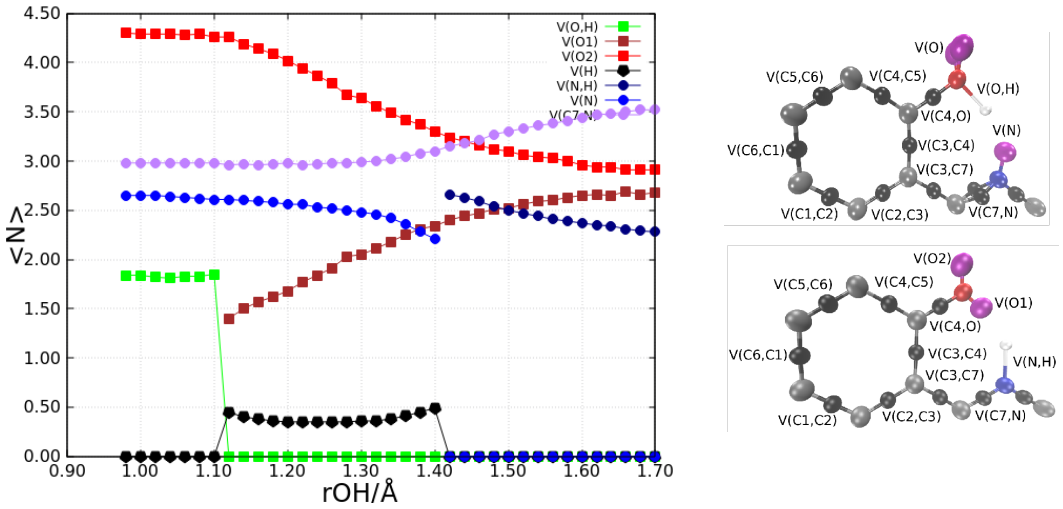

a) b)

Figure 2. a) Variation of the population (in electrons) of the basins of the ELF as a function of the r_{OH} distance (in *Å*) in the proton transfer in the ground state of the SMA. Only the populations of the basins most involved in proton transfer are shown. b) Position of the basins of the SMA at two significant r_{OH} distances: r_{OH}=*0.98 Å,* upper figure, and r_{OH}=*1.70 Å,* lower figure. Gray, red and blue spheres correspond to carbon, oxygen and nitrogen cores respectively. Black spheres match disynaptic basins (bonds). Purple spheres correspond to valence monosynaptic basins V(O1), V(O2), and V(N). A white sphere is used to represent the attractor associated to the V(O,H) basin in the first steps of the reaction, or the V(H) in the intermediate region, or the V(N, H) basin in the keto form.

After the O-H bond breaking, the population of the pseudoatomic form of the proton remains almost constant while the population of new lone-pair of the oxygen (V(O1)) increases and the sum of the number of electron of other two lone-pairs, V(O2), decreases. As the proton-transfer proceeds, the population of the lone-pair of the N, V(N), slightly decreases until the point r_{OH}=*1.40 Å* is reached. At this point, the second catastrophe takes place, corresponding to the formation of the N-H bond. Simultaneously, the V(H) and V(N) basin vanishes, and the new basin associated to the N-H bond, V(N,H), develops. After this point, the essential electronic rearrangements have occurred, but the population of the basins keeps changing. When the keto structure is reached, r_{OH}=*1.70 Å,* the population (bond order) of the V(C7-N) basin has increased by 0.5 *e* compared with the enol. Also, at keto, the population of the three lone-pairs of the O adds up to 5.6 *e*. This unusual highly charged oxygen atom would partially explain why the barrier for the proton transfer in the ground state is high compared with the proton transfer in the excited state, in which there is no barrier. The Coulomb repulsion among these three pair of electrons that build up after the O-H bond breaking can be postulated as the primary physical reason for the high barrier in the ground state. Nonetheless, Rocha et at.[33] postulate that the barrier is a consequence of the loss of aromaticity of the ring. In the Lewis structure of a non-aromatic keto, the expected bond order of the C4-O is 2. However, at the keto, the population of the basin V(C4,O) is only 2 *e*. Nevertheless, this loss of aromaticity is also captured by the ELF as a spreading of the population of the bonds of the ring as the transfer progresses (See Figure S1). In a perfect aromatic ring, all bonds are equivalent. Figure 3 summarizes the changes in topology of the ELF discussed above by depicting the position of the attractors and their populations at significant values of r_{OH}.

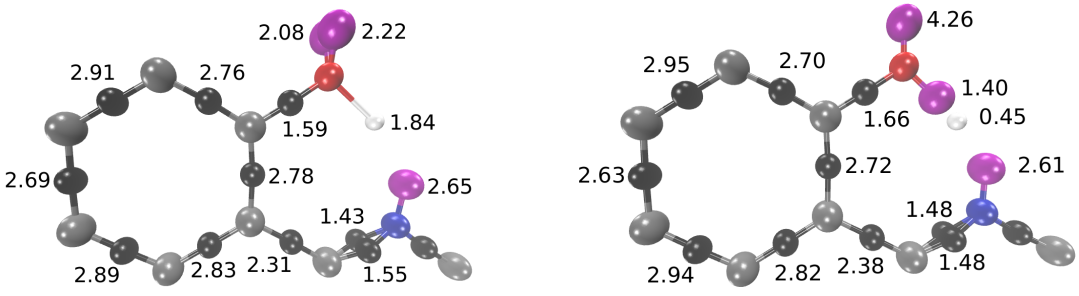

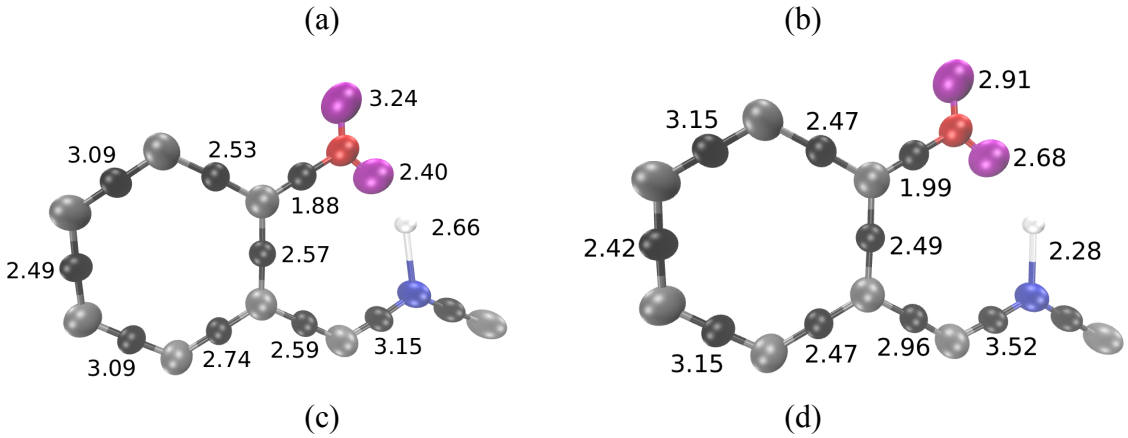

Figure 3. Population and location (speheres) of the basins of the SMA at significant r_{OH} distances (a) r_{OH}=*0.98 Å* (enol) , (b) r_{OH}=*1.12 Å,* (c) r_{OH}=*1.42, Å,* (d) r_{OH}=*1.70 Å* (keto). The color code of the spheres is the same as the one of the Figure 2.

3.2 ***Excited state***.

Similarly to Figure 1, Figure 4 shows excitation energy (S_0 to S_1) along the minimum energy path of the proton transfer and snapshots of localization domain of ELF=0.8 at the enol, keto and what we called the electronic transition state. The jump in energy between the fists two points is because the first corresponds to the Frank-Condon (FC) state, while in second all structural degree of freedom of FC are relaxed but the O-H distance. Despite localization domains in S_0 and S_1 look alike, there are significant differences. First, in S_1 the reaction goes without a barrier. Second, the electronic transition state, and therefore the breaking of the O-H bond, occurs early (r_{OH}=*1.14 Å*) compared to the ground state (r_{OH}=*1.20 Å*). Also, at the keto, a non-bonding monosynaptic basin develops on the N. These features of the topology of the ELF are more natural to discuss with the aid of a plot of the evolution of the population of the basins involved in the proton transfer; Figure 5.

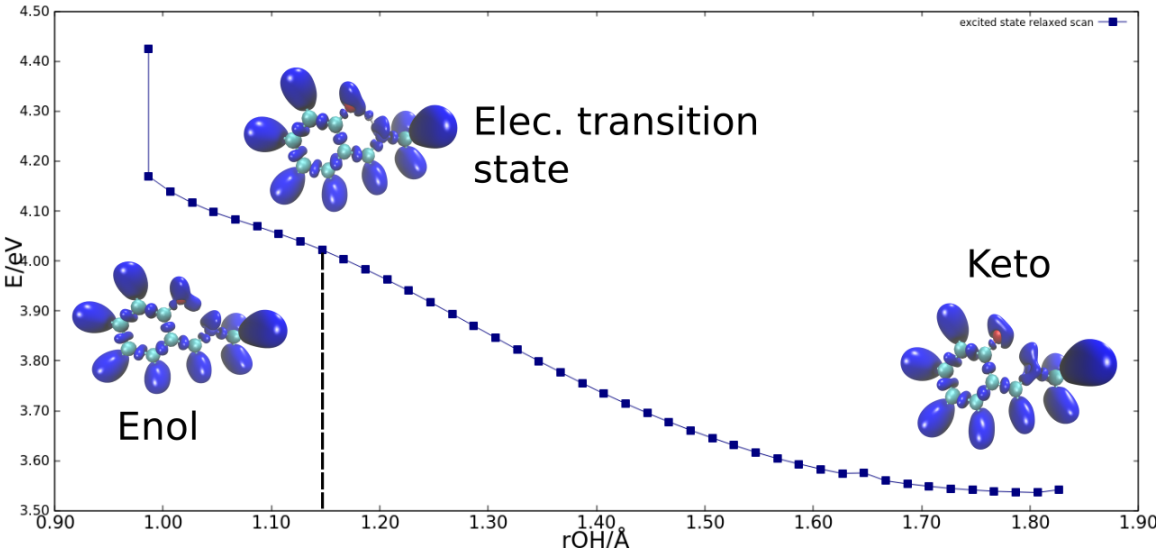

Figure 4. Potential energy surface along the Internal reaction coordinate of the proton transfer in the first singlet excited state of the SMA. Insets are isosurfaces of ELF=0.8. Besides the ELF in the enol and keto, the ELF in the so-called electronic-transition state is also shown. The energy origin corresponds to the energy of the enol tautomer in the ground state.

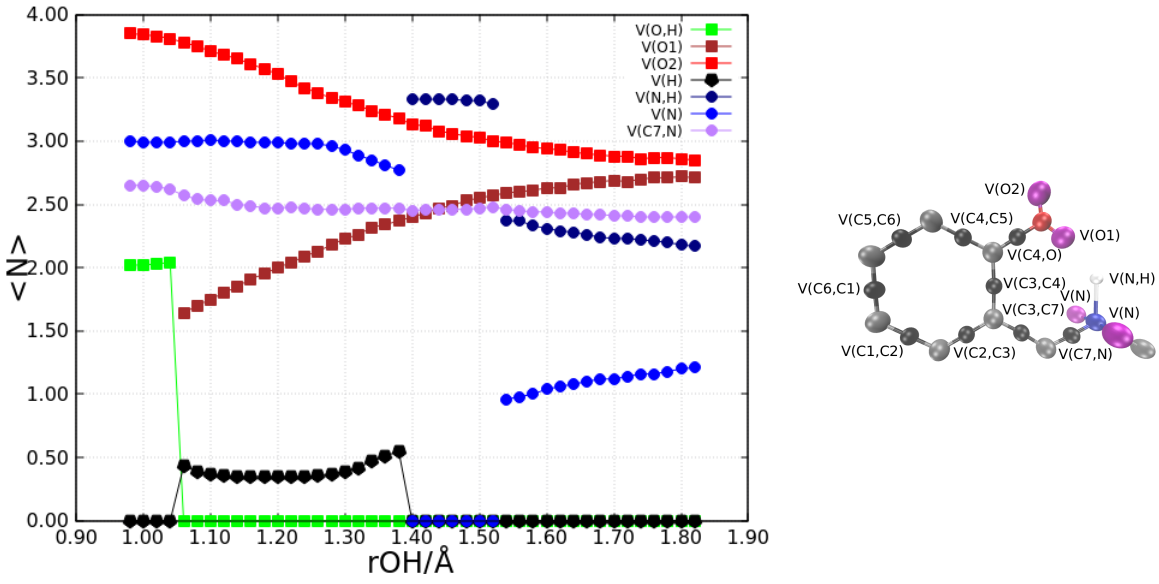

a) b)

Figure 5. a) Variation of the population (in electrons) of the basins of the ELF as a function of the r_{OH} distance (in *Å*) in the proton transfer in the excited state of the SMA. Only the populations of the basins most involved in proton transfer are shown. b) Position of the basins of the SMA at a significant distances (r_{OH}=*0.98 Å*). Gray, red and blue spheres correspond to carbon, oxygen and nitrogen cores respectively. Black spheres match disynaptic basins (bonds). Purple spheres correspond to valence monosynaptic basins V(O1), V(O2), and V(N). A white sphere is used to

represent the attractor associated to the V(O,H) basin in the first steps of the reaction, or the V(H) in the intermediate region, or the V(N, H) basin in the keto form.

In the proton transfer in S_1 three catastrophes occur; one more than in S_0. The first one happens at $r_{OH}=1.06$ *Å,* and it corresponds to the breaking of the O-H bond, V(O,H), the formation of a lone-pair in the Oxygen, V(O1), and the emergence of the pseudoatomic basin of the proton, V(H). From $r_{OH}=1.06$ *Å* to the catastrophe at which the N-H bond is formed ($r_{OH}=1.4$ *Å*), the populations of the basins in S1 are similar to the ones in S0. The only difference is that the population of V(H) prior to the formation of the N-H bond is slightly higher in S_1 (0.55 *e*) than S_0 (0.49 *e*). Right after the excitation (FC), the population of the lone-pair of the N, V(N), is remarkably high (3.0 *e*) compared with the ground state (2.65 e). This excess of electrons in the lone-pair remains constant until a few hundredths of Armstrong before the N-H bond emerges. We believe that the electrostatic attraction between this excess of electrons in the N and the positively charged dressed-proton is the driving force that removes the barrier in the excited state. In other words, the excitation enhances the basicity of the Nitrogen.

Notice that once the N-H bond forms, it inherits the electrons of V(N) and V(H). Hence, the new N-H bond has about 3.5 *e*, which is a substantial excess of charge. This bond persists only in a short range of the energy path (between $r_{OH}=1.4$ *Å* and $r_{OH}=1.5$ *Å*), given rising to three new basins. One of them is a new single N-H bond, V(N-H), with about 2.5 *e*. The others are two new monosynaptic basins on the Nitrogen, whose spatial distribution resembles a p_z atomic orbital. The attractors of these basins form mirror images with the molecular plane (see Figure 6.d), and its populations add up 0.96 *e* at $r_{OH}=1.5$ *Å*, but it increases to 1.2 *e* when the keto is reached. Thus, at the keto form in the excited state, the Nitrogen had roughly one electron in excess in a non-binding basin, which resembles a radical structure. Remarkably, in a recent study of the non-adiabatic dynamics of the proton transfer of the SMA, Barbartti et al.[23] found that at the beginning of the proton transfer, the excitation has π-π character, but it changes to π-n in the same region where the non-bonding basin on the Nitrogen develops.

The excitation also brings a weakening of the C7-N bond, which reveals in the decreasing of the population of the basin V(C7,N) right after the excitation, and as the proton-transfer progresses. While its population at the keto in S_0 is 3.52 *e*, in S_1 is only 2.4 *e*. This reduction of the bond order upon excitation is consistent with the photo-isomerization that may result in the trans-enol form in the ground state (see the left side of the Scheme 1). Figure 6 summarizes the changes in topology of the ELF discussed above by depicting the position of the attractors and their populations at significant values of r_{OH}.

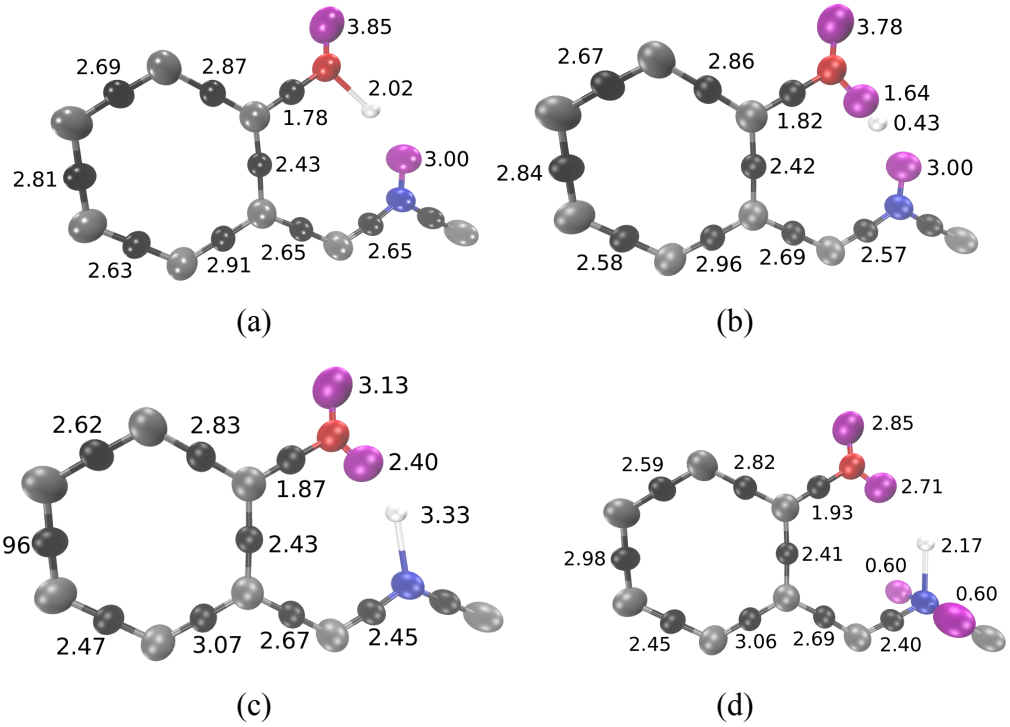

Figure 6. Population and location (spheres) of the basins of the SMA in the excited state at significant r_{OH} distances (a) r_{OH}=*0.98 Å* (enol) , (b) r_{OH}=*1.06 Å,* (c) r_{OH}=*1.40, Å,* (d) r_{OH}=*1.82 Å* (keto). The color code of the spheres is the same as the one of the Figure 2.

A comment on the change of aromaticity of the excited state with the proton transfer is worthy. As we mentioned above, Rocha et al. suggest that the lack of barrier in the excited state is because the proton transfer on it does not reduce the aromaticity of the SMA, in opposition to what occurs in the ground state. We also observe a difference in the aromaticity S_1 and S_0 characterized by the spreading of the population of the bonds of

the ring as the transfer progress (see Figures S1 and S2). Although the persistence of aromaticity in S_1 plays a role in the dynamics of the reaction, we believe that the electrostatic attraction between the proton and the lone electron on the N is the primary driving force of the barrierless photoreaction.

3.3 **Excited-state *proton-transfer dynamics*.**

The proton transfer in the ground state has a barrier (0.31 eV) that it is about half the total vibrational average energy of the whole molecule. If the transfer were to happen, it would do so following a well define internal reaction coordinate that is basically the elongation of O-H bond. However, in the excited state, the lack of barrier makes it more likely that the transference follows other trajectories than the minimum energy path. If this is true, our explanation of the ultrafast transference in terms of the topology of the ELF in S_1 could be not robust enough. It could happen that the discussion of the last subsection would be not valid for all plausible trajectories. To test possible dynamical effects on the topology of the ELF in S_1, we performed a study of the dynamics of the proton transfer using BOMD on the excited state. We computed 20 trajectories as described at the end of the section Computational Methods. For each trajectory, we identify the time at which the proton is at the same distance from the O and N. Then, the time of each trajectory is shifted to that point and the arithmetic mean of the position of atoms of the 20 trajectories is taken. This defines an average trajectory for which the ELF and its topology were evaluated. The populations of the basins of the ELF along the average trajectory are shown in Figure 7. This figure is to compare with Figure 5. It is clear that both plots have the same features and the dynamical effects, such as the out-the-plane movement of the proton does not change the bonding topology. Specifically, the highly charged lone-pair of the nitrogen, V(N), the temporary N-H bond holding 3.5 *e*, V(N,H), and the non-bonding radical basin of the N, are not affected by the vibrational coupling of the O-H-N coordinate with the rest of the molecule. Finally, despite the set up of the molecular dynamics was not intended to characterize the transference-time and its probability of occurrence, our results are in good agreement with other authors. The proton transference-time, measured as the time that takes the proton to sit middle way between the O and N, is 25 ± 8 fs, which agrees with other authors[42-44].

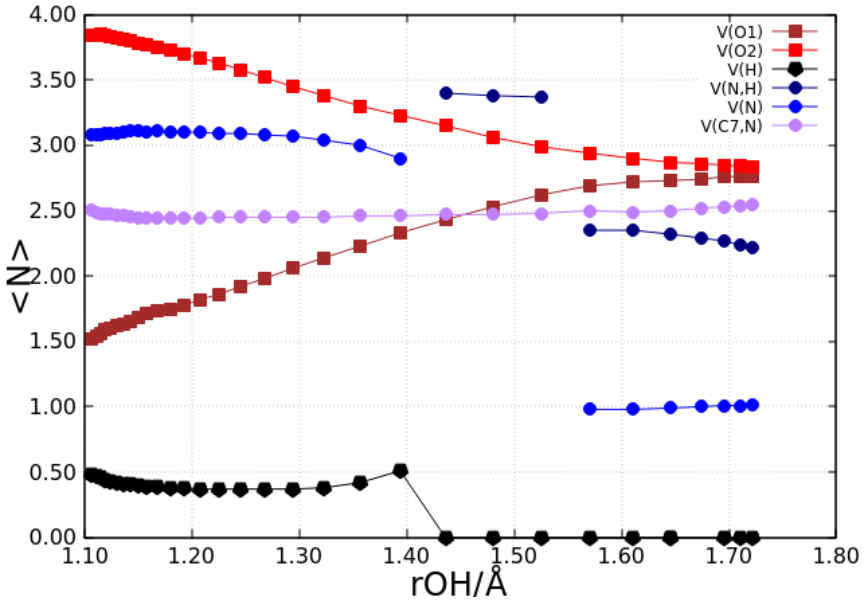

Figure 7. Variation of the population (in electrons) of the basins of the ELF as a function of the r_{OH} distance (in $\AA$) in the proton transfer in the excited state of the SMA. Only the populations of the basins most involved in proton transfer are shown. The labels of the basins are the same as the ones of the Figure 5.

Conclusions.

In this work, two questions have been addressed. One is how to compute the ELF of excited states with the same spin-symmetry as the ground state within TD-DFT. The second is what chemical and physical information reveal the topological analysis of the ELF on the evolution of chemical bonds during the ESIPT in a prototypal Schiff base (the SMA). Equation (4) summarizes our proposal on how to compute the ELF in excited states using the natural orbitals of the 1PDM of the excited state. The main approximation behind Eq. (4) is the HF-like reconstruction of the 2PDM in terms of 1PDM (Eq. (3). The topological analysis of the ELF in the ground state reveals that the proton-transfer is not concerted in the sense that the N-H bond does not create at the same time that the O-H bond breaks. During a short period, the proton exists in a pseudoionic form dressed with half an electron. In the ground state, the breaking of the O-H bond results in the accumulation of three lone-pairs in the oxygen atom. This excess of electrostatic potential energy and the reduction of the aromaticity with proton transfer explain the barriers between enol and ceto forms of the SMA.

The topological analysis of the ELF in the first singlet excited state shows a primary difference in the properties of the lone pair of the N. Right after the excitation the population of this lone-pair reaches *3 e*, which is one electron more than one would expect from Lewis structures. This excess of electrons in the N exerts an electrostatic attraction on the proton and breaks the O-H bond. This excess of electrons can also be interpreted as an enhancement of the basicity of the Nitrogen. Besides, in concordance with previous work,[33] it is observed that in the excited state the reduction of aromaticity from the enol to the ceto is modest compared to the ground state. However, The ELF suggests that the electrostatic attraction between the proton and the lone electron on the N is the primary driving force of the barrierless photoreaction. Also, the ELF shows that after the formation of the N-H bond, the electron in excess in the bond is reallocated in two non-bonding basins located out of the molecular plane. The formation of this non-bonding structure coincides with a change in the type of the excitation (π-π to π-n) recently found by Barbatti et al.[88] in a study of the photodynamics of the SMA.

Because the proton transfer in the excited state goes with no barrier, a minimum energy path might not be a good representation of the paths actually followed by the proton. Hence, we performed Born-Oppenheimer molecular dynamics calculations of the proton transfer in the excited state to check the stability of the topological analysis of the ELF to possible dynamic effects. The topology of an average trajectory is similar to the one of the minimum energy path, which leads us to conclude that, in the SMA, the topological analysis of the ELF in the excited state is robust to fluctuations in geometry that take the reaction path out of planarity.

Finally, the description of the chemical bond, and its dynamics, in excited states using descriptors that depend on the kinetic energy density, deserves further research. It is important for instance, to study the effect of the inclusion of electronic correlation in the reconstruction of the 2-PDM. Descriptors such as the ELF could be useful to shed light on the mechanisms of photochemical reactions and photophysical processes.

Acknowledgments

This work was financed by: i) FONDECYT through projects No 1181121 and 1180623, ii) ECOS C17E09, and iii) Centers Of Excellence With Basal/Conicyt Financing, Grant FB0807. AE acknowledges support form CONICYT for the Ph. D. fellowship 21180073.

REFERENCES.

1. Kawata, S.; Kawata, Y., Three-Dimensional Optical Data Storage Using Photochromic Materials. *Chemical Reviews* **2000,** *100* (5), 1777-1788.
2. Beharry, A. A.; Woolley, G. A., Azobenzene photoswitches for biomolecules. Chemical Society Reviews 2011, 40 (8), 4422-4437.
3. Berkovic, G.; Krongauz, V.; Weiss, V., Spiropyrans and Spirooxazines for Memories and Switches. *Chemical Reviews* **2000,** *100* (5), 1741-1754.
4. Benniston, A. C., Pushing around electrons: towards 2-D and 3-D molecular switches. *Chem. Soc. Rev.* **2004,** *33* (9), 573-578.
5. Raymo, F. M.; Giordani, S., All-optical processing with molecular switches. *Proceedings of the National Academy of Sciences* **2002,** *99* (8), 4941-4944.
6. Padwa, A., Photochemistry of the carbon-nitrogen double bond. *Chemical Reviews (Washington, DC, United States)* **1977,** *77* (1), 37-68.
7. Becker, R. S.; Richey, W. F., Photochromic anils. Mechanisms and products of photoreactions and thermal reactions. *Journal of the American Chemical Society* **1967,** *89* (6), 1298-1302.
8. Zhao, J.; Ji, S.; Chen, Y.; Guo, H.; Yang, P., Excited state intramolecular proton transfer (ESIPT): from principal photophysics to the development of new chromophores and applications in fluorescent molecular probes and luminescent materials. *Phys. Chem. Chem. Phys.* **2012,** *14* (25), 8803-8817.
9. Yin, H.; Li, H.; Xia, G.; Ruan, C.; Shi, Y.; Wang, H.; Jin, M.; Ding, D., A novel non-fluorescent excited state intramolecular proton transfer phenomenon induced by intramolecular hydrogen bonds: an experimental and theoretical investigation. *Scientific Report* **2016,** *6*, 19774/1-19774/9.
10. Vargas, V. C., Time-Resolved Fluorescence of Salicylideneaniline Compounds in Solution. *Journal of Physical Chemistry A* **2004,** *108* (2), 281-288.
11. Ohshima, A.; Momotake, A.; Arai, T., Substituent effects on the ground-state properties of naphthalene-based analogues of salicylideneaniline in solution. *Bulletin of the Chemical Society of Japan* **2006,** *79* (2), 305-311.
12. Ohshima, A.; Momotake, A.; Arai, T., Photochromism, thermochromism, and solvatochromism of naphthalene-based analogues of salicylideneaniline in solution. *Journal of Photochemistry and Photobiology, A: Chemistry* **2004,** *162* (2-3), 473-479.
13. Benelhadj, K.; Muzuzu, W.; Massue, J.; Retailleau, P.; Charaf-Eddin, A.; Laurent, A. D.; Jacquemin, D.; Ulrich, G.; Ziessel, R., White Emitters by Tuning the Excited-State Intramolecular Proton-Transfer Fluorescence Emission in 2-(2'-Hydroxybenzofuran)benzoxazole Dyes. *Chem. - Eur. J.* **2014,** *20* (40), 12843-12857.
14. Zugazagoitia, J. S.; Maya, M.; Damian-Zea, C.; Navarro, P.; Beltran, H. I.; Peon, J., Excited-State Dynamics and Two-Photon Absorption Cross Sections of Fluorescent Diphenyl-TinIV Derivatives with Schiff Bases: A Comparative Study of the Effect of

Chelation from the Ultrafast to the Steady-State Time Scale. *Journal of Physical Chemistry A* **2010,** *114* (2), 704-714.
15. Ziolek, M.; Kubicki, J.; Maciejewski, A.; Naskrecki, R.; Luniewski, W.; Grabowska, A., Unusual conformational effects in proton transfer kinetics of an excited photochromic Schiff base. *Journal of Photochemistry and Photobiology, A: Chemistry* **2006,** *180* (1-2), 101-108.
16. Zhou, P.; Hoffmann, M. R.; Han, K.; He, G., New Insights into the Dual Fluorescence of Methyl Salicylate: Effects of Intermolecular Hydrogen Bonding and Solvation. *J. Phys. Chem. B* **2014,** *119* (6), 2125-2131.
17. Zhong, X. L.; Gao, F.; Wang, Q.; Li, H. R.; Zhang, S. T., Excited state intramolecular proton transfer of novel conjugated derivatives containing hydroxy and imino groups. *Chinese Chemical Letters* **2010,** *21* (6), 1195-1198.
18. Zgierski, M. Z.; Lim, E. C., Photochrome That Was Not: 2-Hydroxynaphtylidene-(8-aminoquinoline). *Journal of Physical Chemistry A* **2011,** *115* (34), 9689-9694.
19. Wang, Q.; Gao, F.; Li, H.; Zhang, S., Photoinduced excited state intramolecular proton transfer of new Schiff base derivatives with extended conjugated chromophores: a comprehensive theoretical survey. *Chinese Journal of Chemistry* **2010,** *28* (6), 901-910.
20. Vargas, V.; Amigo, L., A study of the tautomers of N-salicylidene-p-X-aniline compounds in methanol. *Journal of the Chemical Society, Perkin Transactions 2: Physical Organic Chemistry* **2001,** (7), 1124-1129.
21. Patil, V. S.; Padalkar, V. S.; Tathe, A. B.; Gupta, V. D.; Sekar, N., Synthesis, Photo-physical and DFT Studies of ESIPT Inspired Novel 2-(2',4'-Dihydroxyphenyl)benzimidazole, -benzoxazole and -benzothiazole. *J. Fluoresc.* **2013,** *23* (5), 1019-1029.
22. Padalkar, V. S.; Ramasami, P.; Sekar, N., A Combined Experimental and DFT-TDDFT Study of the Excited-State Intramolecular Proton Transfer (ESIPT) of 2-(2'-Hydroxyphenyl) Imidazole Derivatives. *J Fluoresc* **2013,** *23* (5), 839-851.
23. Jankowska, J.; Barbatti, M.; Sadlej, J.; Sobolewski, A. L., Tailoring the Schiff base photoswitching–a non-adiabatic molecular dynamics study of substituent effect on excited state proton transfer. *Physical Chemistry Chemical Physics* **2017,** *19* (7), 5318-5325.
24. Kwon, J. E.; Park, S. Y., Advanced Organic Optoelectronic Materials: Harnessing Excited-State Intramolecular Proton Transfer (ESIPT) Process. *Advanced Materials* **2011,** *23* (32), 3615-3642.
25. Suzuki, T.; Kaneko, Y.; Arai, T., Photoinduced intramolecular hydrogen atom transfer of N-salicylideneaniline in the triplet state. *Chemistry Letters* **2000,** *29* (7), 756-757.
26. Suzuki, T.; Arai, T., Novel insight into the photochromism and thermochromism of hydrogen bonded Schiff bases. *Chemistry Letters* **2001,** *30* (2), 124-125.
27. Ohshima, A.; Momotake, A.; Arai, T., Photochemistry of salicylideneaniline analogue at low temperature. *Chemistry Letters* **2005,** *34* (9), 1288-1289.
28. Nagaoka, S.; Nagashima, U., Effects of node of wave function upon photochemical reactions of organic molecules. 2. *Journal of Physical Chemistry* **1991,** *95* (10), 4006-4008.
29. Nagaoka, S.-i.; Kusunoki, J.; Fujibuchi, T.; Hatakenaka, S.; Mukai, K.; Nagashima, U., Nodal-plane model of the excited-state intramolecular proton transfer of

2-(o-hydroxyaryl)benzazoles. *Journal of Photochemistry and Photobiology A: Chemistry* **1999,** *122* (3), 151-159.
30. Nagaoka, S.; Nagashima, U.; Ohta, N.; Fujita, M.; Takemura, T., Electronic-state dependence of intramolecular proton transfer of o-hydroxybenzaldehyde. *The Journal of Physical Chemistry* **1988,** *92* (1), 166-171.
31. Nagaoka, S. i.; Nagashima, U., Intramolecular proton transfer in various electronic states of o-hydroxybenzaldehyde. *Chemical Physics* **1989,** *136* (2), 153-163.
32. Nagaoka, S.-i.; Nakamura, A.; Nagashima, U., Nodal-plane model for excited-state intramolecular proton transfer of o-hydroxybenzaldehyde: substituent effect. *Journal of Photochemistry and Photobiology A: Chemistry* **2002,** *154* (1), 23-32.
33. Gutierrez-Arzaluz, L.; Cortes-Guzman, F.; Rocha-Rinza, T.; Peon, J., Ultrafast excited state hydrogen atom transfer in salicylideneaniline driven by changes in aromaticity. *Physical chemistry chemical physics : PCCP* **2015,** *17* (47), 31608-12.
34. Becke, A. D.; Edgecombe, K. E., A simple measure of electron localization in atomic and molecular systems. *Journal of Chemical Physics* **1990,** *92*, 5397-5403.
35. Liu, Y.; Kilby, P.; Frankcombe, T. J.; Schmidt, Timothy W., Electronic transitions of molecules: vibrating Lewis structures. *Chemical Science* **2019**.
36. Richey, W. F.; Becker, R. S., Spectroscopy and mechanisms of the photo- and thermal reactions of photochromic anil. *Journal of Chemical Physics* **1968,** *49* (5), 2092-101.
37. Ziolek, M.; Kubicki, J.; Maciejewski, A.; Naskrecki, R.; Grabowska, A., Excited state proton transfer and photochromism of an aromatic Schiff base. Pico- and femtosecond kinetics of the N,N'-bis(salicylidene)-p-phenylenediamine (BSP). *Chemical Physics Letters* **2003,** *369* (1,2), 80-89.
38. Ziolek, M.; Kubicki, J.; Maciejewski, A.; Naskrecki, R.; Grabowska, A., Enol-keto tautomerism of aromatic photochromic Schiff base N,N'-bis(salicylidene)-p-phenylenediamine: ground state equilibrium and excited state deactivation studied by solvatochromic measurements on ultrafast time scale. *The Journal of chemical physics* **2006,** *124* (12), 124518.
39. Ziolek, M.; Kubicki, J.; Maciejewski, A.; Naskrecki, R.; Grabowska, A., An ultrafast excited state intramolecular proton transfer (ESIPT) and photochromism of salicylideneaniline (SA) and its "double" analogue salicylaldehyde azine (SAA). A controversial case. *Phys. Chem. Chem. Phys.* **2004,** *6* (19), 4682-4689.
40. Randino, C.; Ziolek, M.; Gelabert, R.; Organero, J. A.; Gil, M.; Moreno, M.; Lluch, J. M.; Douhal, A., Photo-deactivation pathways of a double H-bonded photochromic Schiff base investigated by combined theoretical calculations and experimental time-resolved studies. *Physical Chemistry Chemical Physics* **2011,** *13* (33), 14960-14972.
41. Ortiz-Sanchez, J. M.; Gelabert, R.; Moreno, M.; Lluch, J. M., Electronic-structure and quantum dynamical study of the photochromism of the aromatic Schiff base salicylideneaniline. *Journal of Chemical Physics* **2008,** *129* (21), 214308/1-214308/11.
42. Ortiz-Sanchez, J. M.; Gelabert, R.; Moreno, M.; Lluch, J. M., Theoretical Study on the Excited-State Intramolecular Proton Transfer in the Aromatic Schiff Base Salicylidene Methylamine: an Electronic Structure and Quantum Dynamical Approach. *Journal of Physical Chemistry A* **2006,** *110* (14), 4649-4656.

43. Sporkel, L.; Jankowska, J.; Thiel, W., Photoswitching of salicylidene methylamine: a theoretical photodynamics study. *The journal of physical chemistry. B* **2015,** *119* (6), 2702-2710.
44. Spörkel, L.; Cui, G.; Thiel, W., Photodynamics of Schiff Base Salicylideneaniline: Trajectory Surface-Hopping Simulations. *The Journal of Physical Chemistry A* **2013,** *117* (22), 4574-4583.
45. Joshi, H.; Kamounah, F. S.; Gooijer, C.; van, d. Z. G.; Antonov, L., Excited state intramolecular proton transfer in some tautomeric azo dyes and Schiff bases containing intramolecular hydrogen bond. *Journal of Photochemistry and Photobiology A: Chemistry* **2002,** *152* (1-3), 183-191.
46. Koll, A.; Filarowski, A.; Fitzmaurice, D.; Waghorne, E.; Mandal, A.; Mukherjee, S., Excited state proton transfer reaction of two new intramolecularly hydrogen bonded Schiff bases at room temperature and 77K. *Spectrochim Acta A Mol Biomol Spectrosc* **2002,** *58* (1), 197-207.
47. Mandal, A.; Fitzmaurice, D.; Waghorne, E.; Koll, A.; Filarowski, A.; Guha, D.; Mukherjee, S., Ground and excited state proton transfer reaction of two new o-hydroxy Schiff bases in some protic solvents at room temperature and 77 K. *Journal of Photochemistry and Photobiology, A: Chemistry* **2002,** *153* (1-3), 67-76.
48. Jayabharathi, J.; Thanikachalam, V.; Jayamoorthy, K.; Perumal, M. V., A physiochemical study of excited state intramolecular proton transfer process: Luminescent chemosensor by spectroscopic investigation supported by ab initio calculations. *Spectrochimica Acta, Part A: Molecular Spectroscopy* **2011,** *79* (1), 6-16.
49. Jana, S.; Dalapati, S.; Guchhait, N., Proton Transfer Assisted Charge Transfer Phenomena in Photochromic Schiff Bases and Effect of -NEt(2) Groups to the Anil Schiff Bases. *Journal of Physical Chemistry A* **2012,** *116* (45), 10948-10958.
50. Fang, T.-C.; Tsai, H.-Y.; Luo, M.-H.; Chang, C.-W.; Chen, K.-Y., Excited-state charge coupled proton transfer reaction via the dipolar functionality of salicylideneaniline. *Chinese Chemical Letters* **2013,** *24* (2), 145-148.
51. Lin, W.-C.; Fang, S.-K.; Hu, J.-W.; Tsai, H.-Y.; Chen, K.-Y., Ratiometric Fluorescent/Colorimetric Cyanide-Selective Sensor Based on Excited-State Intramolecular Charge Transfer -Excited-State Intramolecular Proton Transfer Switching. *Anal. Chem.* **2014,** *86* (10), 4648-4652.
52. Sekikawa, T.; Schalk, O.; Wu, G.; Boguslavskiy, A. E.; Stolow, A., Initial Processes of Proton Transfer in Salicylideneaniline Studied by Time-Resolved Photoelectron Spectroscopy. *Journal of Physical Chemistry A* **2013,** *117* (14), 2971-2979.
53. Sekikawa, T.; Schalk, O.; Wu, G.; Boguslavskiy, A. E.; Stolow, A., Initial process of proton transfer in salicylideneaniline studied by time-resolved photoelectron spectroscopy. *Journal of Physical Chemsitry A* **2013,** *117* (13), 2971-2979.
54. Luo, M. H.; Tsai, H. Y.; Lin, H. Y.; Fang, S. K.; Chen, K. Y., Extensive spectral tuning of the proton transfer emission from green to red via a rational derivatization of salicylideneaniline. *Chinese Chemical Letters* **2012,** *23* (11), 1279-1282.
55. Sliwa, M.; Naumov, P.; Choi, H.-J.; Nguyen, Q.-T.; Debus, B.; Delbaere, S.; Ruckebusch, C., Effects of a Self-Assembled Molecular Capsule on the Ultrafast Photodynamics of a Photochromic Salicylideneaniline Guest. *ChemPhysChem* **2011,** *12* (9), 1669-1672.

56. Chowdhury, B.; De, R.; Sett, P.; Chowdhury, J., Relaxation of the excited N-(2-hydroxy benzylidene) aniline molecule: An ab initio and TD DFT study. *Journal of Chemical Sciences* **2010,** *122* (6), 857-865.
57. Nakagaki, R.; Kobayashi, T.; Nakamura, J.; Nagakura, S., Spectroscopic and kinetic studies of the photochromism of N-salicylideneanilines and related compounds. *Bull. Chem. Soc. Jpn.* **1977,** *50* (8), 1909-1912.
58. Becker, R. S.; Lenoble, C.; Zein, A., A comprehensive investigation of the photophysics and photochemistry of salicylideneaniline and derivatives of phenylbenzothiazole including solvent effects. *Journal of Physical Chemistry* **1987,** *91* (13), 3509-3517.
59. Barbara, P. F.; Rentzepis, P. M.; Brus, L. E., Photochemical kinetics of salicylidenaniline. *Journal of the American Chemical Society* **1980,** *102* (8), 2786-91.
60. Grabowska, A.; Kownacki, K.; Kaczmarek, L., Proton transfer along the internal hydrogen bonds in excited Schiff bases. Photochromism in symmetric systems with two equivalent reaction sites. *J. Lumin.* **1994,** *60-61*, 886-90.
61. Becker, R. S.; Lenoble, C.; Zein, A., Photophysics and photochemistry of the nitro derivatives of salicylideneaniline and 2-(2'-hydroxyphenyl)benzothiazole and solvent effects. *The Journal of Physical Chemistry* **1987,** *91* (13), 3517-3524.
62. Knyazhansky, M. I.; Metelitsa, A. V.; Bushkov, A. J.; Aldoshin, S. M., Role of structural flexibility in fluorescence and photochromism of the salicylideneaniline: the "aldehyde" ring rotation. *Journal of Photochemistry and Photobiology, A: Chemistry* **1996,** *97* (3), 121-126.
63. Knyazhanskii, M. I.; Makarova, N. I.; Tymyanskii, Y. R.; Kharlanov, V. A., Photoinitated processes in structurally nonrigid molecular systems based on the pyridinium cation and salicylideneaniline molecule. *Zhurnal Prikladnoi Spektroskopii* **1995,** *62* (3), 454-457.
64. Kownacki, K.; Mordzinski, A.; Wilbrandt, R.; Grabowska, A., Laser-induced absorption and fluorescence studies of photochromic Schiff bases. *Chemical Physics Letters* **1994,** *227* (3), 270-6.
65. Rodriguez-Cordoba, W.; Zugazagoitia, J. S.; Collado-Fregoso, E.; Peon, J., Excited State Intramolecular Proton Transfer in Schiff Bases. Decay of the Locally Excited Enol State Observed by Femtosecond Resolved Fluorescence. *Journal of Physical Chemistry A* **2007,** *111* (28), 6241-6247.
66. Gawinecki, R.; Kuczek, A.; Kolehmainen, E.; Osmialowski, B.; Krygowski, T. M.; Kauppinen, R., Influence of Bond Fixation in Benzo-Annulated N-Salicylideneanilines and Their ortho-C(:O)X Derivatives (X = CH3, NH2, OCH3) on Tautomeric Equilibria in Solution. *Journal of Organic Chemistry* **2007,** *72* (15), 5598-5607.
67. Ohshima, A.; Momotake, A.; Arai, T., Substituent effects on the ground-state properties of naphthalene-based analogues of salicylideneaniline in solution. *Bull. Chem. Soc. Jpn.* **2006,** *79* (Copyright (C) 2012 American Chemical Society (ACS). All Rights Reserved.), 305-311.
68. Ohshima, A.; Momotake, A.; Arai, T., Photochemistry of salicylideneaniline analogue at low temperature. *Chem. Lett.* **2005,** *34* (Copyright (C) 2012 American Chemical Society (ACS). All Rights Reserved.), 1288-1289.

69. Okabe, C.; Nakabayashi, T.; Inokuchi, Y.; Nishi, N.; Sekiya, H., Ultrafast excited-state dynamics in photochromic N-salicylideneaniline studied by femtosecond time-resolved REMPI spectroscopy. *Journal of Chemical Physics* **2004,** *121* (19), 9436-9442.
70. Mitra, S.; Tamai, N., Dynamics of photochromism in salicylideneaniline: A femtosecond spectroscopic study. *Phys. Chem. Chem. Phys.* **2003,** *5* (20), 4647-4652.
71. Otsubo, N.; Okabe, C.; Mori, H.; Sakota, K.; Amimoto, K.; Kawato, T.; Sekiya, H., Excited-state intramolecular proton transfer in photochromic jet-cooled N-salicylideneaniline. *Journal of Photochemistry and Photobiology, A: Chemistry* **2002,** *154* (1), 33-39.
72. Suzuki, T.; Arai, T., Novel insight into the photochromism and thermochromism of hydrogen bonded Schiff bases. *Chem. Lett.* **2001,** (Copyright (C) 2012 American Chemical Society (ACS). All Rights Reserved.), 124-125.
73. Ogawa, K.; Harada, J.; Fujiwara, T.; Yoshida, S., Thermochromism of Salicylideneanilines in Solution: Aggregation-controlled Proton Tautomerization. *Journal of Physical Chemistry A* **2001,** *105* (13), 3425-3427.
74. Zgierski, M. Z.; Grabowska, A., Photochromism of salicylideneaniline (SA). How the photochromic transient is created: A theoretical approach. *Journal of Chemical Physics* **2000,** *112* (14), 6329-6337.
75. Suzuki, T.; Kaneko, Y.; Arai, T., Photoinduced intramolecular hydrogen atom transfer of N-salicylideneaniline in the triplet state. *Chem. Lett.* **2000,** (Copyright (C) 2012 American Chemical Society (ACS). All Rights Reserved.), 756-757.
76. Knyazhansky, M. I.; Metelitsa, A. V.; Kletskii, M. E.; Millov, A. A.; Besugliy, S. O., The structural transformations and photo-induced processes in salicylidene alkylimines. *J. Mol. Struct.* **2000,** *526* (1-3), 65-79.
77. Harada, J.; Uekusa, H.; Ohashi, Y., X-ray Analysis of Structural Changes in Photochromic Salicylideneaniline Crystals. Solid-State Reaction Induced by Two-Photon Excitation. *Journal of the American Chemical Society* **1999,** *121* (24), 5809-5810.
78. Mitra, S.; Tamai, N., Femtosecond spectroscopic study on photochromic salicylideneaniline. *Chemical Physics Letters* **1998,** *282* (5,6), 391-397.
79. Zhang, Y.; Zhao, C. Y.; Fang, W. H.; You, X. Z., A molecular design view on the first hyperpolarizability of salicylideneaniline derivatives. *Theoretical Chemistry Accounts* **1997,** *96* (2), 129-134.
80. Sekikawa, T.; Kobayashi, T.; Inabe, T., Femtosecond Fluorescence Study of the Substitution Effect on the Proton Transfer in Thermochromic Salicylideneaniline Crystals. *Journal of Physical Chemistry A* **1997,** *101* (4), 644-649.
81. Sekikawa, T.; Kobayashi, T.; Inabe, T., Femtosecond Fluorescence Study of Proton-Transfer Process in Thermochromic Crystalline Salicylideneanilines. *J. Phys. Chem. B* **1997,** *101* (50), 10645-10652.
82. Kobayashi, T.; Sekikawa, T.; Inabe, T., Femtosecond luminescence study of hydrogen-atom-transfer process in thermochromic crystalline salicylideneanilines. *J. Lumin.* **1997,** *72-74*, 508-510.
83. Kletskii, M. E.; Millov, A. A.; Metelitsa, A. V.; Knyazhansky, M. I., Role of structural flexibility in the fluorescence and photochromism of salicylidene aniline: the general scheme of the photo-transformations. *Journal of Photochemistry and Photobiology, A: Chemistry* **1997,** *110* (3), 267-270.

84. Higelin, D.; Sixl, H., Spectroscopic studies of the photochromism of N-salicylideneaniline mixed crystals and glasses. *Chemical Physics* **1983,** *77* (3), 391-400.
85. Gostev, F. E.; Petrukhin, A. N.; Titov, A. A.; Nadtochenko, V. A.; Sarkisov, O. M.; Metelitsa, A. V.; Minkin, V. I., Intramolecular processes in the excited state of salicylideneaniline-class compounds. *Khimicheskaya Fizika* **2004,** *23* (Copyright (C) 2012 American Chemical Society (ACS). All Rights Reserved.), 3-14.
86. Ziolek, M.; Gil, M.; Organero, J. A.; Douhal, A., What is the difference between the dynamics of anion- and keto-type of photochromic salicylaldehyde azine? *Physical Chemistry Chemical Physics* **2010,** *12* (9), 2107-2115.
87. Sliwa, M.; Mouton, N.; Ruckebusch, C.; Poisson, L.; Idrissi, A.; Aloise, S.; Potier, L.; Dubois, J.; Poizat, O.; Buntinx, G., Investigation of ultrafast photoinduced processes for salicylidene aniline in solution and gas phase. *Photochemical & Photobiological Sciences* **2010,** *9* (5), 661-669.
88. Barbatti, M.; Pittner, J.; Pederzoli, M.; Werner, U.; Mitrić, R.; Bonačić-Koutecký, V.; Lischka, H., Non-adiabatic dynamics of pyrrole: Dependence of deactivation mechanisms on the excitation energy. *Chemical Physics* **2010,** *375* (1), 26-34.
89. Savin, A.; Becke, A. D.; Flad, J.; Nesper, R.; Preuss, H.; Vonschnering, H. G., A New Look at Electron Localization. *Angewandte Chemie* **1991,** *30* (4), 409-412.
90. Silvi, B.; Savin, A., Classification of Chemical-Bonds Based on Topological Analysis of Electron Localization Functions. *Nature* **1994,** *371* (6499), 683-686.
91. Ferro-Costas, D.; Pendás, Á. M.; González, L.; Mosquera, R. A., Beyond the molecular orbital conception of electronically excited states through the quantum theory of atoms in molecules. *Physical Chemistry Chemical Physics* **2014,** *16* (20), 9249-9258.
92. Silvi, B., The spin-pair compositions as local indicators of the nature of the bonding. *The Journal of Physical Chemistry A* **2003,** *107* (17), 3081-3085.
93. Kohout, M., A measure of electron localizability. *International Journal of Quantum Chemistry* **2004,** *97* (1), 651-658.
94. Kohout, M.; Pernal, K.; Wagner, F. R.; Grin, Y., Electron localizability indicator for correlated wavefunctions. I. Parallel-spin pairs. *Theoretical Chemistry Accounts* **2004,** *112* (5), 453-459.
95. Kohout, M.; Pernal, K.; Wagner, F.; Grin, Y., Electron localizability indicator for correlated wavefunctions. II Antiparallel-spin pairs. *Theoretical Chemistry Accounts* **2005,** *113* (5), 287-293.
96. Wagner, F. R.; Bezugly, V.; Kohout, M.; Grin, Y., Charge decomposition analysis of the electron localizability indicator: a bridge between the orbital and direct space representation of the chemical bond. *Chemistry-A European Journal* **2007,** *13* (20), 5724-5741.
97. Notice that not for all methods is possible to construct the 2PD. For instance, this not possible for CCSD and MP(N) but it is for CASSCF and CISD.
98. Casida, M. E.; Chong, D. P., Time-Dependent Density Functional Response Theory for Molecules. In *Recent Advances in Density Functional Methods. Part1.*, World Scientific: Singapore, 1995; pp 155-192.
99. Feixas, F.; Matito, E.; Duran, M.; Solà, M.; Silvi, B., Electron localization function at the correlated level: a natural orbital formulation. *Journal of chemical theory and computation* **2010,** *6* (9), 2736-2742.

100. Pernal, K.; Giesbertz, K. J. H., Reduced Density Matrix Functional Theory (RDMFT) and Linear Response Time-Dependent RDMFT (TD-RDMFT). In *Density-Functional Methods for Excited States*, Ferré, N.; Filatov, M.; Huix-Rotllant, M., Eds. Springer International Publishing: Cham, 2016; pp 125-183.
101. Savin, A.; Silvi, B.; Colonna, F., Topological analysis of the electron localization function applied to delocalized bonds. *Can J Chem* **1996,** *74* (6), 1088-1096.
102. Chai, J.-D.; Head-Gordon, M., Long-range corrected hybrid density functionals with damped atom–atom dispersion corrections. *Phys. Chem. Chem. Phys.* **2008,** *10* (44), 6615-6.
103. Gaussian 09, R. A.; M. J. Frisch, G. W. T., H. B. Schlegel, G. E. Scuseria, M. A. Robb, J. R. Cheeseman, G. Scalmani, V. Barone, B. Mennucci, G. A. Petersson, H. Nakatsuji, M. Caricato, X. Li, H. P. Hratchian, A. F. Izmaylov, J. Bloino, G. Zheng, J. L. Sonnenberg, M. Hada, M. Ehara, K. Toyota, R. Fukuda, J. Hasegawa, M. Ishida, T. Nakajima, Y. Honda, O. Kitao, H. Nakai, T. Vreven, J. A. Montgomery, Jr., J. E. Peralta, F. Ogliaro, M. Bearpark, J. J. Heyd, E. Brothers, K. N. Kudin, V. N. Staroverov, R. Kobayashi, J. Normand, K. Raghavachari, A. Rendell, J. C. Burant, S. S. Iyengar, J. Tomasi, M. Cossi, N. Rega, J. M. Millam, M. Klene, J. E. Knox, J. B. Cross, V. Bakken, C. Adamo, J. Jaramillo, R. Gomperts, R. E. Stratmann, O. Yazyev, A. J. Austin, R. Cammi, C. Pomelli, J. W. Ochterski, R. L. Martin, K. Morokuma, V. G. Zakrzewski, G. A. Voth, P. Salvador, J. J. Dannenberg, S. Dapprich, A. D. Daniels, O. Farkas, J. B. Foresman, J. V. Ortiz, J. Cioslowski, and D. J. Fox, Gaussian, Inc., Wallingford CT, 2009.
104. Noury, S.; Krokidis, X.; Fuster, F.; Silvi, B., Computational tools for the electron localization function topological analysis. *Computers & chemistry* **1999,** *23* (6), 597-604.
105. Heidar-Zadeh, F.; Richer, M.; Fias, S.; Miranda-Quintana, R. A.; Chan, M.; Franco-Pérez, M.; González-Espinoza, C. E.; Kim, T. D.; Lanssens, C.; Patel, A. H. G.; Yang, X. D.; Vöhringer-Martinez, E.; Cárdenas, C.; Verstraelen, T.; Ayers, P. W., An explicit approach to conceptual density functional theory descriptors of arbitrary order. *Chemical Physics Letters* **2016,** *660* (1), 307-312.
106. Silvi, B.; Fourré, I.; Alikhani, M. E., The Topological Analysis of the Electron Localization Function. A Key for a Position Space Representation of Chemical Bonds. *Monatshefte für Chemie / Chemical Monthly* **2005,** *136* (6), 855-879.